

# UC Berkeley

## UC Berkeley Previously Published Works

### Title

Electrically driven light emission from single quantum dots using pulsed MOS capacitors

### Permalink

<https://escholarship.org/uc/item/93x4d0nx>

### Journal

Applied Physics Letters, 123(13)

### ISSN

0003-6951

### Authors

Wang, Vivian

Lin, Qing

Javey, Ali

### Publication Date

2023-09-25





### DOI

10.1063/5.0161775

Peer reviewed

RESEARCH ARTICLE | SEPTEMBER 26 2023

# Electrically driven light emission from single quantum dots using pulsed MOS capacitors

Vivian Wang ; Qing Lin ; Ali Javey  

 Check for updates

*Appl. Phys. Lett.* 123, 131108 (2023)

<https://doi.org/10.1063/5.0161775>



CrossMark



## APL Energy

### Latest Articles Online!

[Read Now](#)



# Electrically driven light emission from single quantum dots using pulsed MOS capacitors

Cite as: Appl. Phys. Lett. **123**, 131108 (2023); doi: [10.1063/5.0161775](https://doi.org/10.1063/5.0161775)

Submitted: 12 June 2023 · Accepted: 3 September 2023 ·

Published Online: 26 September 2023



View Online



Export Citation



CrossMark

Vivian Wang,<sup>1,2</sup>  Qing Lin,<sup>3</sup>  and Ali Javey<sup>1,2,a)</sup> 

## AFFILIATIONS

<sup>1</sup>Electrical Engineering and Computer Sciences, University of California, Berkeley, California 94720, USA

<sup>2</sup>Materials Sciences Division, Lawrence Berkeley National Laboratory, Berkeley, California 94720, USA

<sup>3</sup>Department of Electrical Engineering, Stanford University, Stanford, California 94305, USA

<sup>a)</sup>Author to whom correspondence should be addressed: [ajavey@eecs.berkeley.edu](mailto:ajavey@eecs.berkeley.edu)

## ABSTRACT

Robust, nanoscale light-emitting devices are attractive for emerging photonic and quantum engineering applications. However, conventional approaches suffer from fabrication challenges or lack the potential to address individual nanostructures, such as quantum dots. In this paper, we present a device that can produce electrically driven light emission from a single quantum dot using a single carbon nanotube as the charge injection contact. The device has a metal-oxide-semiconductor capacitor structure and operates based on an unconventional mechanism of electroluminescence, which relies on the use of bipolar voltage pulses. The proposed device can be fabricated in a simple manner using conventional lithographic processes, offering a scalable approach toward the development of optoelectronic devices at the single dot level.

Published under an exclusive license by AIP Publishing. <https://doi.org/10.1063/5.0161775>

Scaling the dimensions of light sources is important for technological applications ranging from augmented reality to quantum science, where electrically driven light emission from micro- to nanoscale devices is desirable.<sup>1–3</sup> In the extreme limit, light emission may be achieved from single semiconductor nanostructures, which could enable compact, electrically triggered single-photon sources.<sup>4,5</sup> However, conventional light-emitting diode (LED) structures can be difficult to scale to ultrasmall dimensions. Devices based on self-assembled quantum dots (QDs) suffer from nonradiative losses owing to deleterious effects of fabrication processes as the active area is scaled down, and it is difficult to design device structures that can selectively inject current in sub-micron active regions.<sup>3</sup> LEDs based on organic materials are typically fabricated using shadow masks, which limits the size of an individual light emitting device to microscale dimensions and precludes the exploration of light emission at the nanoscale. Here, we describe an electroluminescent device structure in which the light emitting region can be scaled from the macroscale to nanoscale with minimal modification of the fabrication process. Using this device, we demonstrate highly reproducible, electrically generated light emission from single colloidal quantum dots using single carbon nanotubes (CNTs) as nanoscale contacts.

Previous work has shown that conventional vertically layered light-emitting diodes can be used to generate light emission from a

collection of single molecules or colloidal quantum dots.<sup>6,7</sup> In these device structures, the emitters are typically embedded in a host matrix at extremely low concentrations, rendering it difficult to control the position of emitters in both the vertical and lateral dimensions due to the finite thickness of the host matrix, which serves as the active layer of the device. The insulating nature of the host matrix also prevents direct and uniform charge injection into the emitters, which can lead to background emission from adjacent material layers in addition to reduced injection efficiency.<sup>8</sup> Furthermore, the sandwiched nature of the device structure hinders efficient optical access and coupling since the emitters are located between two electrode layers. Alternatively, electroluminescence (EL) can be generated from single molecules or nanocrystals using metal electrodes with nanometer-scale gaps,<sup>9,10</sup> but these structures require intricate nanofabrication processes, which typically suffer from poor yield and are difficult to scale reliably. Single-molecule light-emitting devices have been demonstrated using nanoscale gaps between graphene or carbon nanotube electrodes, but positioning a molecule between two separate contacts is challenging.<sup>11,12</sup>

This work presents an alternate strategy using a light-emitting device with a single charge injecting contact. We have previously shown that pulsed-driven, metal-oxide-semiconductor (MOS) capacitors can be used to generate EL from material systems spanning a broad range of dimensions, including molecules, quantum dots,

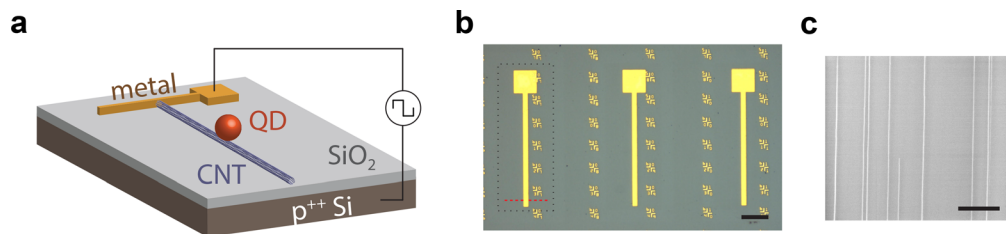


**FIG. 1.** (a) Schematic of a single quantum dot light-emitting device in which pulsed voltage is applied across a capacitor with a carbon nanotube top contact, silicon dioxide dielectric, and silicon back-gate contact. (b) Optical micrograph of several devices fabricated on a substrate with coordinate markers, which serve as a reference for the location of each device across the chip and aid subsequent location of single quantum dots (scale bar:  $100\mu\text{m}$ ). In these devices, carbon nanotubes are oriented perpendicularly to the microfabricated metal electrodes, as indicated by the red dash lines. Carbon nanotubes outside the region near the metal electrode, as indicated by the black dotted lines, are etched away such that each device is electrically isolated. (c) SEM image of individual nanotubes in an aligned carbon nanotube array grown on quartz (scale bar:  $5\mu\text{m}$ ).

nanowires, and two-dimensional semiconductors.<sup>13,14</sup> For films of colloidal quantum dots, bright light emission was demonstrated using capacitors in which networks of CNTs serve as spatially dense nanoscale contacts from which bipolar charge can be injected.<sup>13</sup> Such a device is unique in its requirement for only a single charge injection contact, in contrast to other light-emitting devices, which require separate electron- and hole-injecting contacts with work functions appropriately engineered for the emitting entity. As a result, the emissive layer does not need to be uniform or of any particular thickness, which allows for freeform deposition of emitters. This device concept can, thus, be used to generate EL directly from individual particles placed on a single plane on a silicon substrate.

Figure 1(a) depicts the structure of the two-terminal pulsed electroluminescent device, which consists of semiconductor quantum dots contacting carbon nanotube contacts, which sit atop a silicon dioxide/silicon substrate. The mechanism of such a device has been described previously.<sup>14</sup> During periods of steady-state positive or negative back-gate voltage, negative or positive charge is accumulated in the active material, respectively. When the polarity of the gate voltage rapidly switches sign, the opposite charge carrier is injected before the existing charge carrier in the material can exit, allowing for exciton formation and radiative recombination. Figure 2 shows energy band diagrams extending laterally across the contact-semiconductor interface at different timepoints during this process. At timepoint (i), electrons accumulate in the semiconducting material as expected for a capacitor under positive steady-state DC voltage, where the voltage is applied to the back-gate contact while the top source contact is grounded. At timepoint (ii), the gate voltage instantaneously flips from positive to negative polarity; however, due to the capacitive nature of the device, the voltage is first dropped across the resistive contact-semiconductor interface. Such steep band bending at the contact-semiconductor interface enables tunneling of carriers into the semiconductor. As indicated by the quasi-Fermi levels, a large population of holes tunnels across the Schottky contact, which then recombine with electrons exiting the semiconductor, thereby producing light emission. The opposing process occurs at timepoints (iii) and (iv), in which holes accumulated in the semiconductor recombine with electrons injected by tunneling across downward bending bands at the semiconductor contact. Light emission, thus, occurs transiently after each voltage transition, with a decay time that depends on the material lifetime and device geometry.<sup>15</sup>

Previously, EL was demonstrated with this pulsed MOS capacitor device structure using random networks of single-walled carbon nanotubes as contacts.<sup>13</sup> In this approach, nanotubes are oriented randomly on the substrate during the solution assembly process, with the average density of nanotubes on the surface depending on the self-assembly time. The average nanotube-nanotube spacing in electrically percolating networks is no more than several hundred nanometers as a result of the short lengths of the nanotubes, which are several micrometers long or less.<sup>16,17</sup> In this work, we use aligned arrays of CNTs grown by chemical vapor deposition (CVD) as contacts to the emitters. By tuning the CVD growth process via control of the catalyst thickness, sparsely spaced nanotubes with relatively long lengths can be obtained; a scanning electron microscopy (SEM) image of an as-grown nanotube array on quartz substrate is shown in Fig. 1(c). Using devices

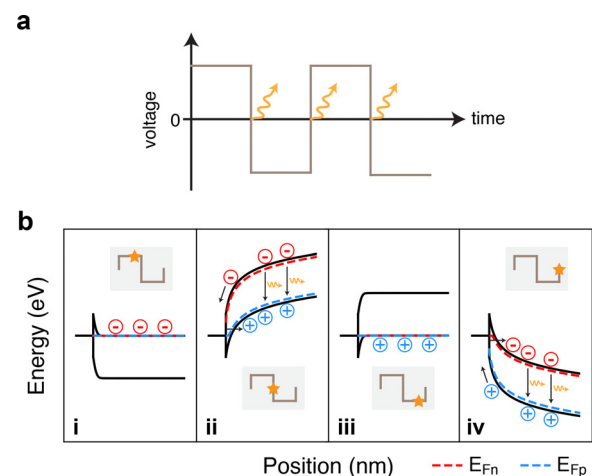


**FIG. 2.** Schematic depicting the operation of a pulsed electroluminescent device at different timepoints of a square wave driving waveform. (a) Light emission occurs at voltage transients with a decay time that depends on material and device properties. (b) Energy band diagrams in each panel illustrate the interface between a charge injecting contact on the left (carbon nanotube) and semiconducting material (quantum dot) on the right. Electrons are accumulated in the semiconductor at time (i), which then exit the semiconductor while holes tunnel in at time (ii), allowing for electron-hole recombination leading to light emission. The reverse process happens at times (iii) and (iv), respectively. The colored dashed lines show the large splitting of electron (red) and hole (blue) quasi-Fermi levels.

fabricated from these nanotube arrays, single quantum dot EL can be observed by widefield imaging.

To briefly summarize the device fabrication process, aligned CNT arrays are first transferred to a silicon dioxide/p<sup>++</sup> silicon substrate via a dry transfer process described in more detail in the supplementary material<sup>18</sup> (Figs. S1 and S2). Metal contacts for wire-bond connections are then patterned and deposited on the CNTs. The active area of the device is defined by a second photolithography step in which CNTs outside the active area are removed by O<sub>2</sub> plasma, thus allowing a device to contact only a single nanotube if so desired. Due to lithographic patterning of the top electrodes, many devices can be fabricated in parallel [Fig. 1(b)]. Finally, emitters are spin-coated on top of the substrate from a solution, which is dilute enough to yield the deposition of isolated single emitters. In this work, we use solution-grown, CdSe-based core-shell quantum dots with peak photoluminescence (PL) emission occurring around 620 nm at room temperature. Device fabrication is completed after the emitter deposition step, and light emission can be observed promptly by applying pulsed voltage between the top metal contact and back-gate p<sup>++</sup> silicon.

The density of light-emitting spots decreases as the concentration of the spin-coated quantum dot solution decreases and as the line density of the aligned carbon nanotube array decreases, due to a fewer number of quantum dots contacting the carbon nanotubes. As shown in Figs. 3(a) and 3(b), discrete spots of EL are observed along individual nanotubes by reducing the density of quantum dots deposited. Based on atomic force microscopy (AFM) and PL measurements, the areal density of quantum dots on the substrate is found to vary linearly with concentration of the spin-coated solution, allowing control of the average number of dots deposited on the surface of the device. As the QD concentration is reduced, the PL signal decreases linearly with QD concentration until there is on average no more than

one QD excited by the laser. For relatively dilute QD deposition, the number of quantum dots deposited in a small region of the substrate would be approximately Poisson distributed. From correlated AFM and widefield photoluminescence imaging, we can identify the location of single quantum dots [Fig. S3(a)], for which a representative photoluminescence spectrum at room temperature is shown in Fig. S3(c).

By spin-coating an appropriately dilute concentration of quantum dots and applying a square wave driving waveform across the device, we can observe EL from single isolated spots. Many of these spots exhibit intensity fluctuations in which the emission turns on and off transiently over time [Fig. 4(f)], as illustrated by successive frames of electroluminescence images captured in real time [Fig. 3(c)]. In this example, we observe electroluminescence from different quantum dots contacting a single nanotube which turn on and off as time elapses. The emission intermittency suggests that these spots represent emission from single quantum dots, which are known to exhibit characteristic “blinking” at the single dot level due to non-radiative Auger processes.<sup>19,20</sup> In general, the yield of these devices is high: EL from similarly dilute QD solution was observed from every device tested so long as carbon nanotubes were properly transferred to the region of the substrate where the devices were fabricated and measured.

The density of single quantum dot emission spots in this scheme depends on the likelihood of a quantum dot landing on a CNT. In a purely random deposition process in which there is an average of  $N_Q$  dots (of diameter 20 nm) in a  $\mu\text{m}^2$  region on a substrate with a line density of  $\rho_C$  nanotubes per  $\mu\text{m}$ , the probability that at least one quantum dot lands on a nanotube is roughly  $1 - (1 - p)^{N_Q}$ , where  $p = \rho_C/50$  is the probability of a quantum dot landing on a nanotube, assuming each dot is deposited independently of one another and ignoring size exclusion effects. This event occurs with 50% probability if  $N_Q = 11 \mu\text{m}^{-2}$  when  $\rho_C = 3 \mu\text{m}^{-1}$  for example. When this event happens, we have the opportunity to observe quantum dot EL, although individual quantum dots are not necessarily resolvable in optical imaging. The probability of having no more than one dot-on-nanotube per  $1 \mu\text{m}$  length across the axis of the aligned CNT array is  $(1 - p)^{N_Q} + N_Q p (1 - p)^{N_Q - 1} \approx 86\%$  for the same parameters. For an aligned CNT array with a sparser line density of  $\rho_C = 0.1 \mu\text{m}^{-1}$ , the probability of having the opportunity for EL is 2% and the probability of having no more than one dot-on-nanotube is 99.97%. By imaging fifty  $1 \mu\text{m}^2$  areas, one spot with possible EL might be expected, and the spot would be extremely likely to represent emission from a single quantum dot. In practice, the QD spin-coating process may not yield uniformly random QD locations as QDs could be more or less likely to deposit on CNTs depending on the surface chemistry, biasing the optimal concentration for observing single quantum dot emission.

Operating characteristics of the device are shown in Fig. 4. The emission intensity from individual dots increases, on average, with the peak voltage applied to the device, as well as the slew rate and frequency of the pulsed waveform [Fig. 4(e)], in correspondence with previous work on pulsed electroluminescence from MOS capacitor devices.<sup>15</sup> It should be noted that the exact shape of the modulated waveform applied at the quantum dot device depends on RC parasitics and bandwidth of the equipment connections. Based on these trends, we operated a device with a custom circuit board in which moderately high voltage pulses can be applied with a faster slew rate than that of the function generator and voltage amplifier used earlier. Images of electroluminescence from the device driven under these conditions

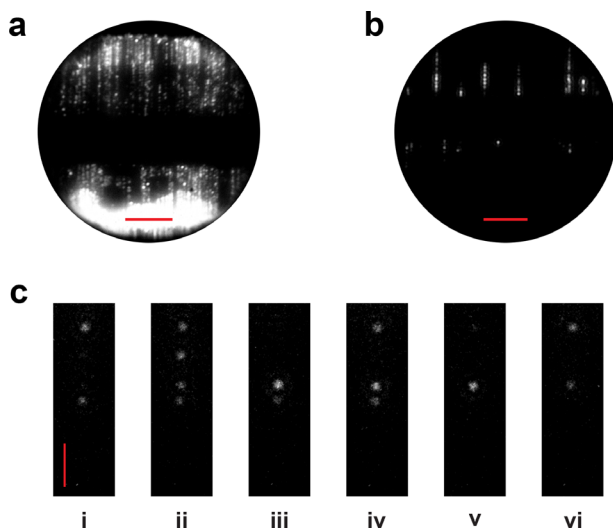


**FIG. 3.** Electroluminescence images of devices with (a) high and (b) low quantum dot surface density on an aligned array of carbon nanotubes. (c) Electroluminescence images captured over time show multiple blinking quantum dot emission spots along a single carbon nanotube. The acquisition time of each image is 1 s. A subset of the continuously acquired images is shown in a chronological order from panel i to vi, with time intervals on the order of seconds. Scale bars:  $20 \mu\text{m}$ .

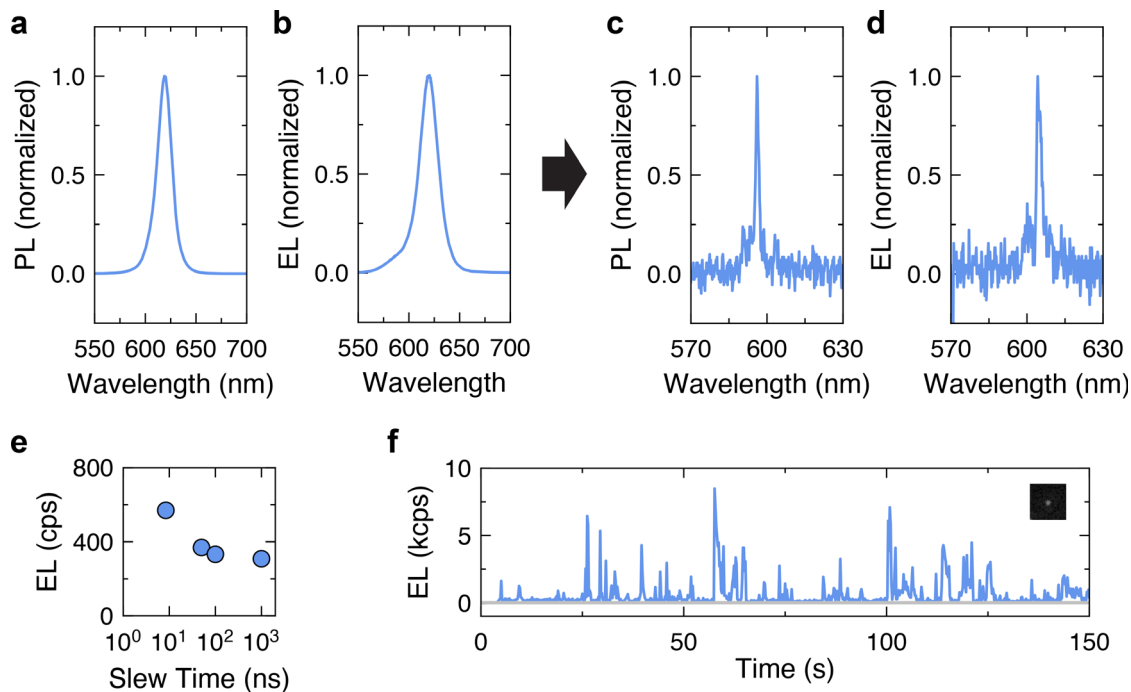


**FIG. 4.** (a) Photoluminescence and (b) electroluminescence spectrum of a film of quantum dots at room temperature. (c) Photoluminescence and (b) electroluminescence spectrum of single quantum dots at cryogenic temperature. (e) Electroluminescence intensity for varying slew time of a square wave gate voltage applied from a function generator. The data point at  $10^3$  ns slew time corresponds to sine wave excitation. (f) Fluctuation in electroluminescence intensity as a function of time for the emitting spot shown in the inset.

show that it is possible to obtain quantum dot emission using supply voltages of only several volts (Fig. S4). It has been previously shown that electroluminescence can be obtained from single molecules using alternating current voltages in which the electron and hole injection processes are temporally separated; however, the device was fabricated in a highly specific manner to the emitting material investigated (Ag nanoclusters) and exhibits poor spectral control with broad and highly variable emission spectra.<sup>21,22</sup>

Quantum dot electroluminescence can be obtained from pulsed MOS capacitor devices at temperatures ranging from room temperature down to cryogenic temperatures. At low temperature (near 4 K), we captured the spectrum of emission from a single blinking spot and found a fairly sharp electroluminescence spectrum with a narrowed linewidth typical of single quantum dot emission [Fig. 4(d)].<sup>23,24</sup> The electroluminescence spectrum is consistent with measurements of single quantum dot photoluminescence spectra at cryogenic temperature [Fig. 4(c)] and is also noticeably sharper than other single-dot electroluminescence spectra previously reported in the literature.<sup>6</sup> For comparison, in a device with an ensemble film of quantum dots, the electroluminescence spectrum remains broad from room temperature down to cryogenic temperatures due to inhomogeneous broadening from polydispersity in the colloiddally synthesized solution of quantum dots [Figs. 4(a), 4(b), and S5]. Finally, we performed AFM imaging on the devices to verify physically the presence of single quantum dots on carbon nanotubes, which yield emission spots. To aid the location of specific emission points from electroluminescence imaging, the silicon dioxide/silicon substrate on which the devices are fabricated is pre-

patterned with a grid of gold markers [Fig. 1(b)]. Each marker's numbers denote its horizontal and vertical position on the chip, which allows for more precise registration of images captured from different sources and easier correlation between AFM and optical imaging of quantum dots. Figure S6 shows the electroluminescence image of a single emitting spot as well as the corresponding AFM image from that region. A quantum dot is found along the CNT from which electroluminescence is observed, thus confirming that EL can be obtained from single quantum dots using single CNT contacts.

In summary, the device platform presented in this work presents a means by which electrically driven light emission can be achieved from nanoscale emitters down to single particles. While here we focus on large core-shell quantum dots with visible emission, the device could be extended to study emission from different quantum dots emitting at other wavelengths, as well as other luminescent entities like single molecules for which molecular optoelectronic devices are difficult to construct or rely on highly specific chemistry or emission physics.<sup>25</sup> The ability to perform single-particle measurements may also reveal information useful to the design of micro- and macro-scale light-emitting devices with ensemble films, including correlations between quantum yield, lifetime, and blinking in individual nanocrystals under the influence of high electric fields, heating, charging, and other effects.<sup>26–28</sup> Careful statistical characterization of heterogeneity in individual nanocrystal properties could guide routes of future material and device optimization.<sup>29,30</sup> For example, the dependence of EL on the sequence of positive or negative voltage transitions can provide information about electron and hole charge injection processes<sup>31</sup> (Fig. S7).

From an engineering perspective, such a platform opens up plentiful opportunities for design of integrated nanoscale light-emitting devices in the future. For instance, single quantum dots could be deterministically placed on single carbon nanotube contacts in order to achieve light emission from defined, localized spots in a scalable manner and avoid the current method of probabilistic fabrication. Regular arrays of single quantum dots with desired spatial patterns could be envisaged, opening up avenues toward the fabrication of unusually designed optoelectronic devices at the nanoscale.<sup>32</sup> Since no processing steps are required after deposition of the luminescent material, single particle emitters could be patterned through a variety of top-down or bottom-up techniques.<sup>33,34</sup> A relatively simpler approach might be to deposit a monolayer of quantum dots on top of an insulating masking layer patterned by e-beam lithography, in which the masking layer contains line openings of nanometer-scale width in which only single quantum dots can contact the underlying CNT. Because the device is patterned by conventional and mature lithographic processes, the locations of carbon nanotube contacts can be defined beforehand, thereby pre-constraining the emission locations along a single lateral dimension and allowing the active area to be easily defined to individual nanotubes. As such, the device provides a viable route toward individually addressable, electrically excited point emitters, unlike other approaches, which use microscale or larger electrical contacts and cannot inject current into only a single quantum dot due to the inability to confine electrical current at nanoscale dimensions.<sup>6,7</sup> Finally, exploration of higher order properties of light emission (e.g., single-photon purity) from these devices could inform their potential functional use for photonic quantum technologies and other yet to be explored optoelectronic applications.<sup>4,35</sup>

See the supplementary material for Figs. S1–S6 and description of experimental methods.

This work was funded by the U.S. Department of Energy, Office of Science, Office of Basic Energy Sciences, Materials Sciences and Engineering Division under Contract No. DE-AC02-05-CH11231 (EMAT program KC1201). The authors thank H.-S. Philip Wong for assistance with carbon nanotube samples.

## AUTHOR DECLARATIONS

### Conflict of Interest

The authors have no conflicts to disclose.

### Author Contributions

**Vivian Wang:** Conceptualization (equal); Investigation (equal); Methodology (equal); Writing – original draft (equal); Writing – review & editing (equal). **Qing Lin:** Investigation (supporting); Methodology (supporting); Resources (equal). **Ali Javey:** Conceptualization (equal); Funding acquisition (equal); Methodology (equal); Supervision (equal); Writing – review & editing (equal).

### DATA AVAILABILITY

The data that support the findings of this study are available within the article and its supplementary material.

## REFERENCES

- T. Meng, Y. Zheng, D. Zhao, H. Hu, Y. Zhu, Z. Xu, S. Ju, J. Jing, X. Chen, H. Gao, K. Yang, T. Guo, F. Li, J. Fan, and L. Qian, “Ultra-high-resolution quantum-dot light-emitting diodes,” *Nat. Photonics* **16**, 297–303 (2022).
- W.-J. Joo, J. Kyoung, M. Esfandyarpour, S.-H. Lee, H. Koo, S. Song, Y.-N. Kwon, S. H. Song, J. C. Bae, A. Jo, M.-J. Kwon, S. H. Han, S.-H. Kim, S. Hwang, and M. L. Brongersma, “Metasurface-driven OLED displays beyond 10,000 pixels per inch,” *Science* **370**, 459–463 (2020).
- A. Fiore, J. X. Chen, and M. Illegems, “Scaling quantum-dot light-emitting diodes to submicrometer sizes,” *Appl. Phys. Lett.* **81**, 1756–1758 (2002).
- I. Aharonovich, D. Englund, and M. Toth, “Solid-state single-photon emitters,” *Nat. Photonics* **10**, 631–641 (2016).
- C. R. Kagan, L. C. Bassett, C. B. Murray, and S. M. Thompson, “Colloidal quantum dots as platforms for quantum information science,” *Chem. Rev.* **121**, 3186–3233 (2021).
- X. Lin, X. Dai, C. Pu, Y. Deng, Y. Niu, L. Tong, W. Fang, Y. Jin, and X. Peng, “Electrically-driven single-photon sources based on colloidal quantum dots with near-optimal antibunching at room temperature,” *Nat. Commun.* **8**, 1132 (2017).
- M. Nothaft, S. Höhla, F. Jelezko, N. Frühauf, J. Pflaum, and J. Wrachtrup, “Electrically driven photon antibunching from a single molecule at room temperature,” *Nat. Commun.* **3**, 628 (2012).
- H. Huang, A. Dorn, V. Bulovic, and M. G. Bawendi, “Electrically driven light emission from single colloidal quantum dots at room temperature,” *Appl. Phys. Lett.* **90**, 023110 (2007).
- A. Dorn, H. Huang, and M. G. Bawendi, “Electroluminescence from nanocrystals in an electromigrated gap composed of two different metals,” *Nano Lett.* **8**, 1347–1351 (2008).
- M. S. Gudiksen, K. N. Maher, L. Ouyang, and H. Park, “Electroluminescence from a single-nanocrystal transistor,” *Nano Lett.* **5**, 2257–2261 (2005).
- C. W. Marquardt, S. Grunder, A. Błaszczak, S. Dehm, F. Hennrich, H. V. Löhneysen, M. Mayor, and R. Krupke, “Electroluminescence from a single nanotube-molecule-nanotube junction,” *Nat. Nanotechnol.* **5**, 863–867 (2010).
- C. Yang, Y. Guo, S. Zhou, Z. Liu, Z. Liu, D. Zhang, and X. Guo, “A tunable single-molecule light-emitting diode with single-photon precision,” *Adv. Mater.* **35**, e2209750 (2023).
- Y. Zhao, V. Wang, D.-H. Lien, and A. Javey, “A generic electroluminescent device for emission from infrared to ultraviolet wavelengths,” *Nat. Electron.* **3**, 612–621 (2020).
- D.-H. Lien, M. Amani, S. B. Desai, G. H. Ahn, K. Han, J.-H. He, J. W. Ager, 3rd, M. C. Wu, and A. Javey, “Large-area and bright pulsed electroluminescence in monolayer semiconductors,” *Nat. Commun.* **9**, 1229 (2018).
- V. Wang, Y. Zhao, and A. Javey, “Performance limits of an alternating current electroluminescent device,” *Adv. Mater.* **33**, e2005635 (2021).
- L. Hu, D. S. Hecht, and G. Grüner, “Percolation in transparent and conducting carbon nanotube networks,” *Nano Lett.* **4**, 2513–2517 (2004).
- M. S. Arnold, S. I. Stupp, and M. C. Hersam, “Enrichment of single-walled carbon nanotubes by diameter in density gradients,” *Nano Lett.* **5**, 713–718 (2005).
- M. R. Rosenberger, M. C. Wang, X. Xie, J. A. Rogers, S. Nam, and W. P. King, “Measuring individual carbon nanotubes and single graphene sheets using atomic force microscope infrared spectroscopy,” *Nanotechnology* **28**, 355707 (2017).
- A. L. Efros and D. J. Nesbitt, “Origin and control of blinking in quantum dots,” *Nat. Nanotechnol.* **11**, 661–671 (2016).
- C. Galland, Y. Ghosh, A. Steinbrück, M. Sykora, J. A. Hollingsworth, V. I. Klimov, and H. Htoon, “Two types of luminescence blinking revealed by spectroelectrochemistry of single quantum dots,” *Nature* **479**, 203–207 (2011).
- T.-H. Lee, J. I. Gonzalez, and R. M. Dickson, “Strongly enhanced field-dependent single-molecule electroluminescence,” *Proc. Natl. Acad. Sci. U. S. A.* **99**, 10272–10275 (2002).
- T.-H. Lee and R. M. Dickson, “Single-molecule LEDs from nanoscale electroluminescent junctions,” *J. Phys. Chem. B* **107**, 7387–7390 (2003).
- S. A. Empedocles, D. J. Norris, and M. G. Bawendi, “Photoluminescence spectroscopy of single CdSe nanocrystallite quantum dots,” *Phys. Rev. Lett.* **77**, 3873–3876 (1996).

- <sup>24</sup>S. A. Empedocles, R. Neuhauser, K. Shimizu, and M. G. Bawendi, "Photoluminescence from single semiconductor nanostructures," *Adv. Mater.* **11**, 1243 (1999).
- <sup>25</sup>T.-H. Lee, J. I. Gonzalez, J. Zheng, and R. M. Dickson, "Single-molecule optoelectronics," *Acc. Chem. Res.* **38**, 534–541 (2005).
- <sup>26</sup>J. Zhou, A. I. Chizhik, S. Chu, and D. Jin, "Single-particle spectroscopy for functional nanomaterials," *Nature* **579**, 41–50 (2020).
- <sup>27</sup>Y. Honmou, S. Hirata, H. Komiyama, J. Hiyoshi, S. Kawauchi, T. Iyoda, and M. Vacha, "Single-molecule electroluminescence and photoluminescence of polyfluorene unveils the photophysics behind the green emission band," *Nat. Commun.* **5**, 4666 (2014).
- <sup>28</sup>D. K. Sharma, S. Hirata, and M. Vacha, "Single-particle electroluminescence of CsPbBr<sub>3</sub> perovskite nanocrystals reveals particle-selective recombination and blinking as key efficiency factors," *Nat. Commun.* **10**, 4499 (2019).
- <sup>29</sup>Y. Ebenstein, T. Mokari, and U. Banin, "Fluorescence quantum yield of CdSe/ZnS nanocrystals investigated by correlated atomic-force and single-particle fluorescence microscopy," *Appl. Phys. Lett.* **80**, 4033–4035 (2002).
- <sup>30</sup>Y. Deng, X. Lin, W. Fang, D. Di, L. Wang, R. H. Friend, X. Peng, and Y. Jin, "Deciphering exciton-generation processes in quantum-dot electroluminescence," *Nat. Commun.* **11**, 2309 (2020).
- <sup>31</sup>L. P. Keating, H. Lee, S. P. Rogers, C. Huang, and M. Shim, "Charging and charged species in quantum dot light-emitting diodes," *Nano Lett.* **22**, 9500–9506 (2022).
- <sup>32</sup>A. Gopinath, C. Thachuk, A. Mitskovets, H. A. Atwater, D. Kirkpatrick, and P. W. K. Rothemund, "Absolute and arbitrary orientation of single-molecule shapes," *Science* **371**, eabd6179 (2021).
- <sup>33</sup>W. Xie, R. Gomes, T. Aubert, S. Bisschop, Y. Zhu, Z. Hens, E. Brainis, and D. Van Thourhout, "Nanoscale and single-dot patterning of colloidal quantum dots," *Nano Lett.* **15**, 7481–7487 (2015).
- <sup>34</sup>H. Zhang, C. Kinnear, and P. Mulvaney, "Fabrication of single-nanocrystal arrays," *Adv. Mater.* **32**, e1904551 (2020).
- <sup>35</sup>K. Hoshino, A. Gopal, M. S. Glaz, D. A. Vanden Bout, and X. Zhang, "Nanoscale fluorescence imaging with quantum dot near-field electroluminescence," *Appl. Phys. Lett.* **101**, 043118 (2012).